ChemComm

Accepted Manuscript

This article can be cited before page numbers have been issued, to do this please use: Y. Wang, D. Gao, P. Zhang, P. Gong, C. Chen, G. Gao and L. Cai, *Chem. Commun.*, 2013, DOI: 10.1039/C3CC47649A.

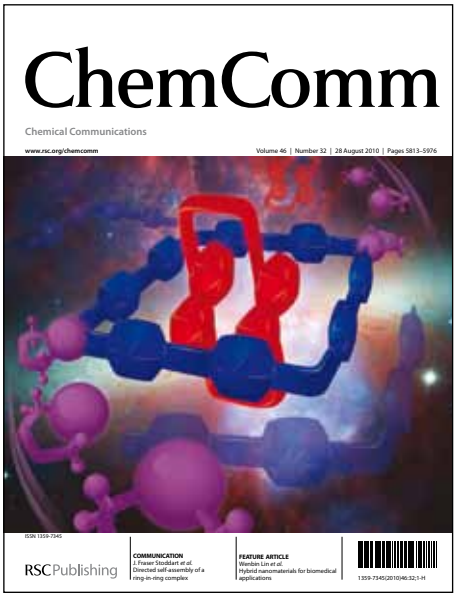

This is an *Accepted Manuscript*, which has been through the RSC Publishing peer review process and has been accepted for publication.

Accepted Manuscripts are published online shortly after acceptance, which is prior to technical editing, formatting and proof reading. This free service from RSC Publishing allows authors to make their results available to the community, in citable form, before publication of the edited article. This *Accepted Manuscript* will be replaced by the edited and formatted *Advance Article* as soon as this is available.

To cite this manuscript please use its permanent Digital Object Identifier (DOI®), which is identical for all formats of publication.

More information about *Accepted Manuscripts* can be found in the **Information for Authors**.

Please note that technical editing may introduce minor changes to the text and/or graphics contained in the manuscript submitted by the author(s) which may alter content, and that the standard **Terms & Conditions** and the **ethical guidelines** that apply to the journal are still applicable. In no event shall the RSC be held responsible for any errors or omissions in these *Accepted Manuscript* manuscripts or any consequences arising from the use of any information contained in them.

Cite this: DOI: 10.1039/c0xx00000x

www.rsc.org/xxxxxx

View Article Online
DOI: 10.1039/C3CC47649A

ARTICLE TYPE

Near infrared fluorescence resonance energy transfer based aptamer biosensor for insulin detection in human plasma

Yuhui Wang, Duyang Gao, Pengfei Zhang, Ping Gong, Chi Chen, Guanhui Gao and Lintao Cai*

Received (in XXX, XXX) Xth XXXXXXXXX 20XX, Accepted Xth XXXXXXXXX 20XX
DOI: 10.1039/b000000x

A new FRET model with near-infrared quantum-dots (NIR-QDs) and oxidized carbon nanoparticles (OCNPs) as the energy donor and acceptor was constructed and designed for insulin detection in complex human plasma.

Fluorescence resonance energy transfer (FRET) has been paid increased attention in various fields like immunoassay, nucleic acid hybridization and interaction of biomacromolecules due to its fascinating merits, such as high sensitivity, noninvasive and homogeneous assay, which is built on the nonradiative energy transfer from the luminescent donor to the acceptor via dipole-dipole interaction within short proximity (1 ~ 10 nm).[1] Unfortunately, FRET based on spectroscopic technology involves in some native drawbacks in optical spectroscopy, for instance, the auto-fluorescence and scattered light from biological matrix, and the co-excitation of the donor and the acceptor since the overlap of their excitation spectra.[2] Obviously, these optical shortcomings lower the sensitivity of FRET assay, especially in complicated biological samples. Additionally, the sensitivity is tightly associated with the optical properties of the donor and the acceptor, as well as the energy transfer efficiency.[3] Therefore, it is meaningful to seek new FRET model with fine-selected donor-acceptor pair to avoid the above-mentioned optical interference and to improve analytical performance in bioassay.

Typically, autofluorescence and scattered light can be greatly reduced in NIR detection window (650 ~ 900 nm). Thus, FRET with detection window in NIR range kindly open the new opportunity to overcome the problems.[4] NIR-QDs have been verified to be efficient and promising energy donor due to their excellent photophysical properties (high quantum yield, large-Stokes shift and weak photobleaching),[5] which was firstly explored by Zhu's group,[3b] and further developed by Xia and Kong.[6] As to the acceptor, NIR organic dyes inevitably suffer from quite a few deficiencies such as weak stability, high cost and difficult synthesis, and thus are rarely applied in NIR-FRET. Recent years, gold nanorods have attracted increasing attention in FRET because of their outstanding surface plasma resonance absorption capacity in NIR range,[7] which have been gradually utilized in the aforementioned NIR-QDs-based FRET sensors. Nonetheless, surface modification and biological label are obligatorily needed in gold acceptor, resulting in time-consuming and complicated procedures in some degree.[8] Recently, carbon nanoparticles (CNPs) has been gradually utilized as a competitive acceptor in FRET because of its superquenching capacity and self-assembly with ssDNA by the π-π stacking interaction.[9] Compared with frequently-used two-dimensional graphene acceptor, CNPs is zero-dimensional and possesses obvious merits such as uniform size distribution, easy synthesis and good compatibility with biomolecules.[3c,9b,9d] Furthermore, CNPs show wide absorption range from ultraviolet to NIR,[3c] and may be capable of promising acceptor candidate to NIR-QDs.

Herein, we firstly report a new FRET architecture employing NIR-QDs and OCNPs as the donor-acceptor pair and insulin as the model analyte. The principle is illustrated in Scheme 1. Insulin aptamer as a selected linker is covalently anchored on the surface of NIR-QDs, which effectively bound with OCNPs through the π–π interaction, leading to shortened distance between the donor and the acceptor. As a result, FRET from NIR-QDs to OCNPs naturally occurs and the fluorescence of the donor is suppressed. When insulin is subjected to the sensor, the QDs-aptamer-OCNPs complex is decomposed because of the weakened π – π interaction between aptamer and OCNPs, which is mainly attributed to the high affinity of insulin towards aptamer. Thus, the process of FRET is inhibited and the fluorescence of NIR-QDs is restored in an insulin concentration-related method. It can be seen that the FRET system is facilely fabricated because only one label step is involved. Furthermore, the detection window of this FRET is in NIR range (750 nm), where the autofluorescence and scattered light arising from biological matrix are greatly avoided, ensuring high sensitivity of the sensor.

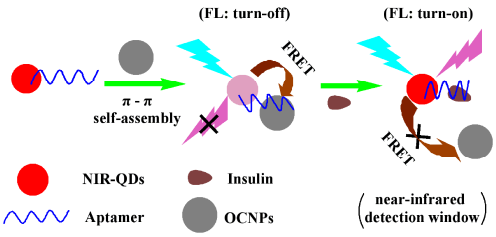

Scheme 1. Schematic illustration of insulin aptamer biosensor based on FRET from NIR-QDs to OCNPs (not to real scale).

To realize this design, NIR-QDs and OCNPs were prepared severally (details in ESI) according to our previous report.[10] As shown in Fig. S1, the TEM image shows that QDs with diameter ca. 8 nm exhibits good monodispersibility and uniform size distribution. The appearance of the unique peaks of Se, Te, Cd, Zn, S in EDX spectrum demonstrates the formation of CdTeSe/ZnS QDs. The FT-IR spectrum of PMAH-coated QDs

shows typical absorption peaks of methylene asymmetric and symmetric C−H stretching (2959-2860 cm^{-1}), C=O stretching (1686 cm^{-1}), asymmetric and symmetric COO^- stretching (1391 cm^{-1}), C-O stretching (1196-1138 cm^{-1}), which approve successful functionalization of PMAH on the surface of QDs. The quantum yield (QY) of PMAH-QDs was tested and calculated as ca. 0.4 according to the literature,[11] which was competitive compared with organic fluorescent dyes. The photoluminescence (PL), UV-vis and FT-IR spectra were performed to verify successful conjugation between QDs and aptamer. In Fig. S2A, about 4 nm red shift of the PL emission peak is found in QDs-aptamer, which may be attributed to the decrease of confinement in one dimension.[12] And the fluorescence quenching of QDs after the conjugation was ascribed to the mechanism of electron spin exchange or electron transfer.[13] The UV-vis absorption peak of aptamer at 260 nm was also obtained in QDs-aptamer (inset in Fig. S2A). FT-IR spectrum of QDs-aptamer was measured (Fig. S2B), and compared with that of QDs (Fig. S1C), unique absorption peaks of DNA at 1098, 990 cm^{-1} were observed in QDs-aptamer bioconjugates.[14] The results have clearly confirmed the successful conjugation between aptamer and QDs.

In Fig. S3A, the TEM photo indicates that OCNPs shows approximately spherical morphology with a diameter distribution ranging from 40 to 60 nm. As compared to graphene or graphene oxide with nonuniform size distribution from nanometers to micrometers, OCNPs is uniform in size and may be more suitable for stable fluorescence quenching. Fig. S3B shows the UV-vis absorption spectrum of OCNPs, which exhibits quite wide absorption from ultraviolet to NIR (200-850 nm), ensuring good overlap with the NIR emission of QDs. The inset of Fig. S3B indicates that the as-prepared OCNPs are water-soluble because of the appearance of hydrophilic groups through the oxidization procedure. Such broad absorption and good water-solubility make OCNPs a competitive nano-quencher for various donors.

To build the FRET-based biosensor, the ratio of the donor to acceptor and the incubation time were optimized. As shown in Fig. 1A, the fluorescence of QDs-aptamer (0.072 mg/mL) sharply decreases along with the addition of OCNPs from 0 to 0.03 mg/mL. The maximum quenching efficiency is about 75.2% and reaches a platform with further elevated concentrations of OCNPs. In Fig S4, the TEM image shows that QDs-aptamer is bound on the surface of OCNPs. The average hydrodynamic sizes of QDs-aptamer, OCNPs, QDs (without aptamer conjugated) plus OCNPs, and QDs-aptamer-OCNPs compound were characterized by dynamic light scattering (DLS) (Fig S5), and the results clearly illustrated that only QDs-aptamer could bind with OCNPs, leading to an increase in size. A control experiment was performed to prove that the fluorescence quenching of QDs was induced by the self-assembly between aptamer and OCNPs. In Fig 1B, it can be seen that the fluorescence of QDs (not aptamer linked) decreases about 3% after the addition of OCNPs. The results visily demonstrate that tiny non-specific quenching occurred, and the most fluorescence quenching of QDs was mainly attributed to the aptamer-linked FRET process from the donor to the acceptor, which was distinctly affirmed by the next fluorescence lifetime experiment. The fluorescence lifetimes of QDs-aptamer and the complex of QDs-aptamer-OCNPs were measured and calculated as ca. 20.5 and 5.3 ns, respectively (Fig S6). And the transfer efficiency (E, 74.1%) was obtained according to the typical equation i.e. $E = 1- \tau_{DA}/\tau_D$ (τ_D and τ_{DA} represent the fluorescence lifetime of the donor in the absence and prescence of the acceptor, respectively),[15] which was consistent with the maxtrum quenching efficiency. In Fig. S7, the fluorescence quenching efficiency reached maximum and kept in consistency after 1 h incubation. Thus, fixed concentrations of the donor and the acceptor (QDs-aptamer: 0.072 mg/mL, OCNPs: 0.03 mg/mL) were applied to construct the sensor, and 1 h incubation was adopted to ensure full quenching and stable background for the following sensing.

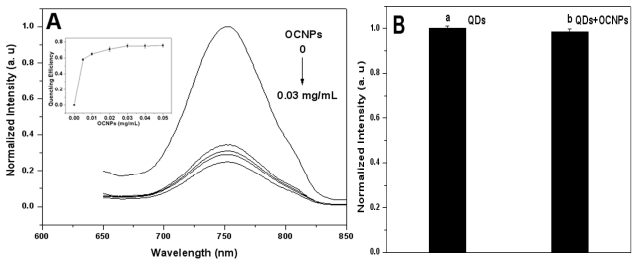

Fig. 1 (A) FL quenching of QDs-aptamer toward varying concentrations of OCNPs. Inset: quenching efficiency versus various amounts of OCNPs (0, 0.005, 0.01, 0.02, 0.03, 0.04, 0.05 mg/mL). (B) FL intensity (at 750 nm) of QDs in the absence and presence of OCNPs.

In the process of detection, the time curve of fluorescence restoration was firstly investigated and shown in Fig. S8, which affirms that the fluorescence reached maximum recovery in 1 h incubation and kept stable with longer incubation. As shown in Fig. 2A, the donor fluorescence of the sensor increases gradually with the constant addition of insulin. In Fig. 2B, a linear curve is found between the fluorescence restoration and the concentration of insulin ranging from 1 pM to 2.0 nM. The fluorescence recovery reached a platform when higher concentration of insulin was added (inset in Fig. 2B). The detection window of the sensor was in NIR range, where the autofluorescence and scattered light were eliminated in great degree, resulting in higher S/N ratio and sensitivity. Furthermore, OCNPs own outstanding fluorescence quenching ability, and thus high quenching efficiency was obtained, leading to low background for fluorescence restoration, which was also a factor for the improvement of sensitivity. Therefore, this sensor could detect insulin as low as 0.6 pM, which was a competitive sensitivity compared with that obtained by other insulin assays.[16] This sensor was designed on the basis of homogeneous FRET technology, which completely avoided tedious washing and separation steps in the heterogeneous assays.[16a,16b] In addition, the influence of QDs tagged with different concentrations of aptamer on the analytical performance of the sensor was investigated. As shown in Table S1, relatively low quenching efficiency and unsatisfying detection limit are obtained if QDs modified with low concentration of aptamer, which may be attributed to the incomplete binding between QDs and OCNPs. However, QDs modified with more aptamer might gain greater opportunities to be preferentially bound with OCNPs by the π–π interaction, leading to elevated quenching efficiency, and thus higher sensitivity is naturally achieved. Nonetheless, QDs labeled with too high concentration of aptamer (above 7.5 nM) is not beneficial to improving the sensitivity, which is probably a result from the saturation of quenching efficiency.

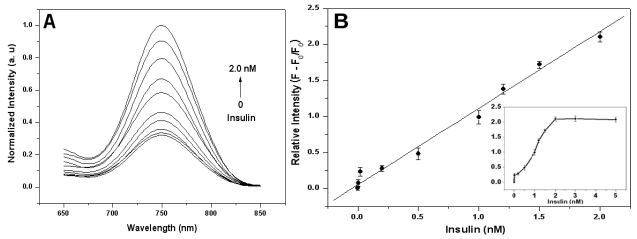

Fig. 2 (A) FL recovery of the sensor towards various concentrations of insulin (0, 0.001, 0.005, 0.02, 0.2, 0.5, 1.0, 1.2, 1.5, 2.0 nM). (B) Linear relationship between fluorescence enhancement and the concentration of insulin. Inset: relation curve of fluorescence enhancement and the concentration range of insulin.

In order to verify the selectivity of the sensor for insulin, numerous interfering substance including ions, amino acids and proteins were studied. As shown in Fig. 3, no obvious fluorescence enhancement induced by these substances (0.1 μM) is observed, while only 2.0 nM of insulin results in great increment of fluorescence. The results thus clearly show high selectivity of the sensor.

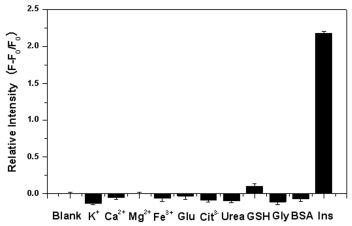

Fig. 3 Relative intensity ($F–F_0/F_0$) of the sensor versus different inspected species, where F_0 represents the fluorescence intensity of the sensor (blank), and F is the intensity of the mixture plus interfering substance.

After that, the sensor was employed to detect the insulin level in human plasma to verify its applicability in biological matrix. Firstly, the autofluorescence of human plasma (20-fold dilution) was measured. In Fig. S9A, obvious visible fluorescence is observed in diluted plasma, while the fluorescence in NIR range is rarely found. Thus, great optical interference of FRET emerges in the visible detection window. Furthermore, the influence of human plasma on the fluorescence of QDs-aptamer is illustrated in Fig. S9B, which indicates that the human plasma shows no obvious effect on fluorescence spectrum and the emission intensity at 750 nm of QDs-aptamer. Thus, the sensor can be used for insulin sensing directly in human plasma without optical interference. Thereafter, five clinical human plasma samples were subjected and measured with the results listed in Table S2. Taking the 20-fold dilution into account, the insulin levels of the samples were from 62 to 74 pM with a RSD within 5%, in according with that measured by other assays.[16a,16c] Then, standard addition experiments were performed to validate the proposed method. The recoveries were from 72% to 116%, which were acceptable for clinical assay. The results exhibit high robustness of this NIR-FRET-based sensor in complex matrix.

In conclusion, a new FRET system was firstly built using NIR-QDs and OCNPs as the donor-acceptor pair, and designed for insulin sensing. This FRET model fully utilized the optical merits of NIR-QDs, the superquenching ability of OCNPs and the high specificity of aptamer, and thus good analytical performances were obtained. The sensor was successfully applied to detect insulin directly in human plasma without optical interference. Furthermore, this sensor could be developed to build up sensing platform through linking various aptamers or other ligands.

View Article Online
DOI: 10.1039/C3CC47649A

The presented work was financially supported by the National Basic Research Program of China (Grant No. 2011CB933600), the National Natural Science Foundation of China (Grant No. 21305152) and the Natural Science Foundation of Guangdong (Grant No. S2013040014454).

Notes and references

CAS Key Laboratory of Health Informatics, Guangdong Key Laboratory of Nanomedicine, Shenzhen Key Laboratory of Cancer Nanotechnology, Institute of Biomedicine and Biotechnology, Shenzhen Institutes of Advanced Technology, Chinese Academy of Sciences, Shenzhen, 518055, P. R.. China. E-mail: lt.cai@siat.ac.cn

† Electronic Supplementary Information (ESI) available: [details of any supplementary information available should be included here]. See DOI: 10.1039/b000000x/

1 (a) K. E. Sapsford, L. Berti and I. L. Medintz, *Angew. Chem., Int. Ed*, 2006, **45**, 4562; (b) S. Wang, N. Mamedova, N. A. Kotov, W. Chen and J. Studer, *Nano Lett*, 2002, **2**, 817.

2 (a) L. Liu, M. Shao, X. Dong, X. Yu, Z. Liu, Z. He and Q. Wang, *Anal. Chem*, 2008, **80**, 7735; (b) K. Kuningas, T. Rantanen, T. Ukonaho, T. Lövgren and T. Soukka, *Anal. Chem*, 2005, **77**, 7348; (c) D. W. Willard, L. L. Carillo, J. Jung and A. V. Orden, *Nano Lett*, 2001, **1**, 469.

3 (a) Y. Wang, Z. Wu and Z. Liu, *Anal. Chem*, 2013, **85**, 258; (b) G. X. Liang, H. C. Pan, Y. Li, L. P. Jiang, J. R. Zhang and J. J. Zhu, *Biosens. Bioelectron*, 2009, **24**, 3693; (c) Y. Wang, L. Bao, Z. Liu and D. Pang, *Anal. Chem*, 2011, **83**, 8130.

4 (a) S. Zhang, V. Metelev, D. Tabatadze, P. C. Zamecnik and A. Bogdanov Jr, *Proc. Natl. Acda. Sci. USA*, 2008, **105**, 4156; (b) Y. Zhang, Y. Li and X. P. Yan, *Anal. Chem*, 2009, **81**, 5001.

5 Q. Ma and X. Su, *Analyst*, 2010, **136**, 1867.

6 (a) Y. Xia, L. Song and C. Zhu, *Anal. Chem*, 2011, **83**, 1401; (b) Q. Zeng, Y. Zhang, X. Liu, L. Tu, X. Kong and H. Zhang, *Chem. Commun*, 2012, **48**, 1781.

7 (a) B. Nikoobakht and M. A. El-Sayed, *Chem. Mater*, 2003, **15**, 1957; (b) C. J. Murphy, A. M. Gole, S. E. Hunyadi, J. W. Stone, P. N. Sisco, A. Alkilany, B. E. Kinard and P. Hankins, *Chem. Commun*, 2008, 544.

8 (a) C. H. Lu, H. H. Yang, C. L. Zhu, X. Chen and G. N. Chen, *Angew. Chem., Int. Ed*, 2009, **48**, 4785; (b) H. Zhang, F. Li, B. Dever, X. F. Li and X. C. Le, *Chem. Rev*, 2013, **113**, 2812.

9 (a) H. Li, Y. Zhang, L. Wang, J. Tian and X. Sun, *Chem. Commun*, 2011, **47**, 961; (b) X. Ouyang, J. Liu, J. Li and R. Yang, *Chem. Commun*, 2012, **48**, 88; (c) Y. Wang, P. Shen, C. Li, Y. Wang and Z. Liu, *Anal. Chem*, 2012, **84**, 1466; (d) L. Zeng, Y. Yuan, P. Shen, K. Y. Wong and Z. Liu, *Chem. Eur. J*, 2013, **19**, 8063.

10 (a) D. Hu, P. Zhang, P. Gong, S. Lian, Y. Lu, D. Gao and L. Cai, *Nanoscale*, 2011, **3**, 4724; (b) P. Zhang, S. Liu, D. Gao, D. Hu, P. Gong, Z. Sheng, J. Deng, Y. Ma and L. Cai, *J. Am. Chem. Soc*. 2012, **134**, 8388.

11 T. Pons, N. Lequeux, B. Mahler, S. Sasnouski, A. Fragola and B. Dubertret, *Chem. Mater*, 2009, **21**, 1418.

12 J. Li, M. Xu, H. Huang, J. Zhou, E. S. Abdel-Halimb, J. R. Zhang and J. J. Zhu, *Talanta*, 2011, **85**, 2113.

13 Z. Tang, N. A. Kotov and M. Giersig, *Science*, 2002, **297**, 237.

14 E. M. Giacobbe, Q. Mi, M. T. Colvin, B. Cohen, C. Ramanan, A. M. Scott, S. Yeganeh, T. J. Marks, M. A. Ratner and M. R. Wasielewski, *J. Am. Chem. Soc*, 2009, **131**, 3700.

15 J. R. Lakowicz, Principles of Fluorescence Spectroscopy, 3rd ed, Springer, 2006, 446.

16 (a) L. Andersen, B. Dinesen, P. N. Jorgensen, F. Poulsen and M. E. Roder, *Clin. Chem*, 1993, **39**, 578; (b) X. Luo, M. Xu, C. Freeman, T. James and J. J. Davis, *Anal. Chem*, 2013, **85**, 4129; (c) H. Iwase, M. Kobayashi, M. Nakajima and T. Takatori, *Forensic. Sci. Int*, 2001, **115**, 123; (d) Y. Pu, Z. Zhu, D. Han, H. Liu, J. Liu, J. Liao, K. Zhang and W. Tan, *Analyst*, 2011, **136**, 4138.